Karlsruher Institut für Technologie

Horizon2020
European Union Funding
for Research & Innovation

electronic transport and the hydrodynamic approach

Boris Narozhny

Institute for Theoretical Condensed Matter Physics, KIT

thanks to my collaborators I. Aleiner, P. Alekseev, U. Briskot, S. Danz, A. Dmitriev, I. Gornyi, V. Kachorovskii, E. Kiselev, J. Link, A. Mirlin, M. Titov, J. Schmalian, M. Schütt, D. Sheehy

DFG

FLAG-ERA

electronic transport

key experimental tool to study electronic properties of solids

standard linear response theory – bulk systems

phenomenological description of transport properties reflecting the observed linear relation between the driving bias and measured response

Ohm's Law

Ziman (1962)

electric and heat currents

$$\boldsymbol{J} = \sigma \boldsymbol{E} - \sigma\alpha \boldsymbol{\nabla} T$$

$$\boldsymbol{Q} = \sigma\alpha T \boldsymbol{E} - (\kappa + \sigma\alpha^2 T) \boldsymbol{\nabla} T$$

Drude formula

$$\sigma = \frac{e^2 n \tau}{m^*}$$

thermal conductivity

$$\kappa = \frac{\pi^2 T}{3e^2} \sigma$$

thermoelectric power

$$\alpha = \frac{\pi^2 T}{3e} \frac{1}{\sigma} \left. \frac{\partial \sigma}{\partial \epsilon} \right|_{\epsilon = E_F}$$

Hall coefficient

$$R_H = \frac{1}{nec}$$

Wiedemann-Franz Law

Ziman (1962)

Lorentz number

$$L = \frac{\kappa}{\sigma T} \quad \Rightarrow \quad L_0 = \frac{\pi^2}{3e^2}$$

copper

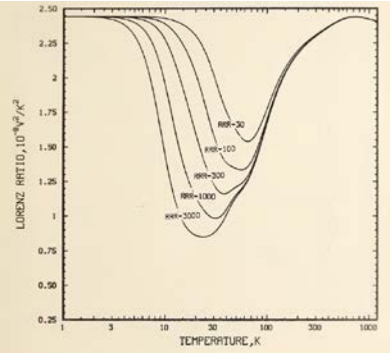

National Bureau of Standards (1984)

temperature dependence of electrical resistivity: “conventional” metals

typical experiments measure resistivity as a function of temperature and magnetic field

copper (engineer’s view)

Springer Handbook (2017)

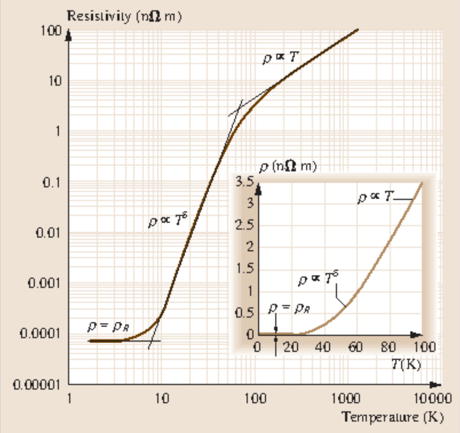

$$E_F = 7\,\mathrm{eV}$$

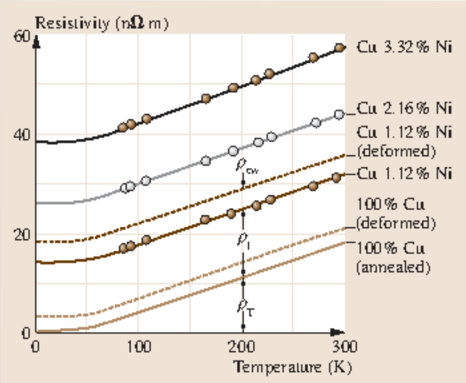

$$\rho(T > T_D) \propto T$$

2D electron systems in heterostructures

Spivak et.al. RMP (2010)

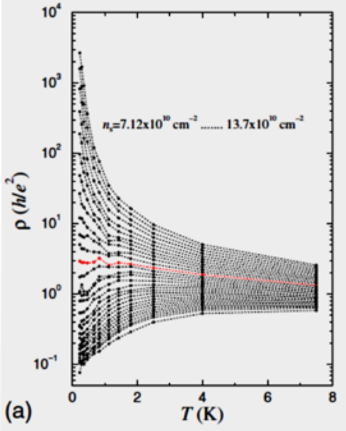

$$T_F \approx 7\,\mathrm{K}$$

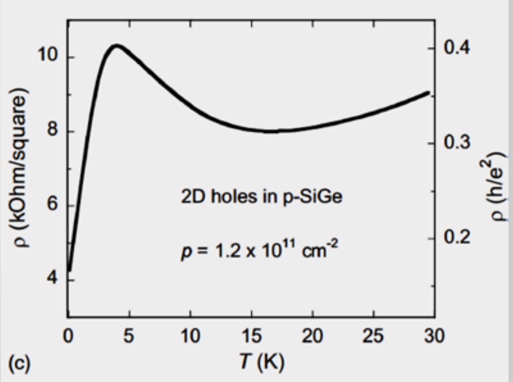

$$E_F = \frac{\pi n}{2m^*} \approx 0.58\,\mathrm{eV}$$

at

$$n = 10^{11}\,\mathrm{cm}^{-2}$$

hydrodynamics

macroscopic theory describing long-wavelength behavior of a fluid as a manifestation of conservation laws

Galilean-invariant fluids

Landau, Lifshitz, vols. 6, 10

Poiseuille flow

Poiseuille (1840)

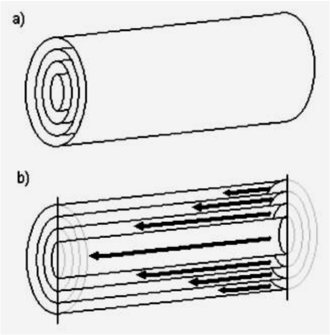

$$\nabla p = \eta \Delta \boldsymbol{v}$$

$$u_z = -\frac{\partial p}{\partial z} \frac{R^2 - r^2}{4\eta}$$

$$u_r = u_\theta = 0$$

$$I = \frac{\pi n R^4}{8 \eta l} \delta p$$

incompressible fluid

no-slip boundary conditions

parabolic velocity profile

Poiseuille flow in the presence of obstacles

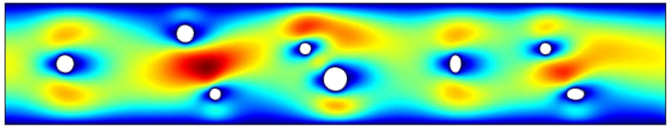

flows around obstacles avoiding scattering

flow rate exceeding independent molecular flow (Knudsen flow)

key to understand superballistic transport experiments in graphene

electronic hydrodynamics

is it possible for electrons to exhibit collective transport?

Gurzhi effect

transition from Knudsen to Poiseuille flow in clean, narrow samples

resistance minimum

Gurzhi (1963)

$\ell_{ee} \ll d$

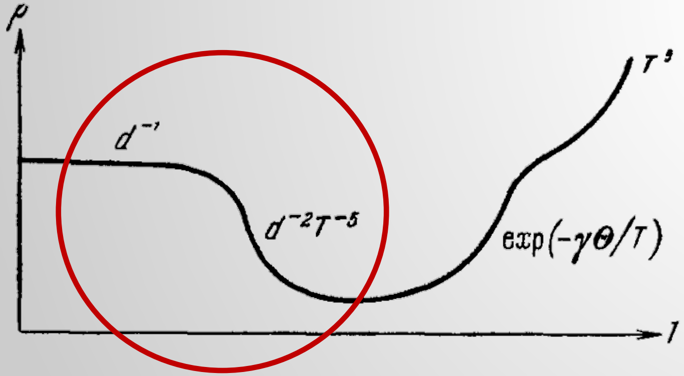

non-monotonic differential conductance

de Jong, Molenkamp (1995)

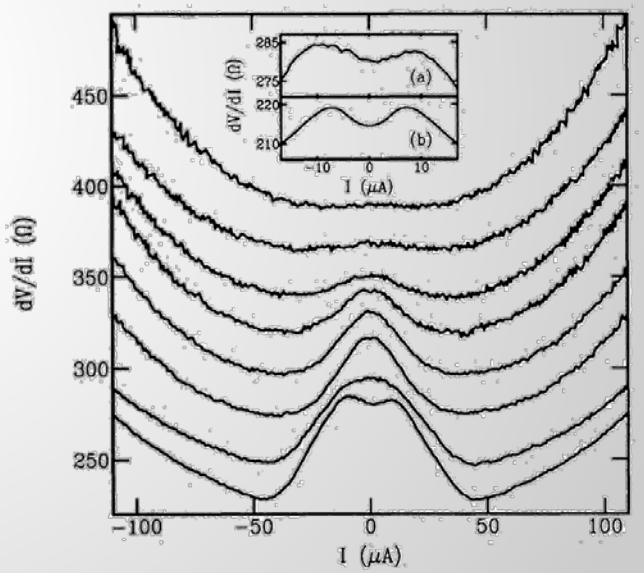

why is it so hard for electrons to behave collectively?

unlike fluid molecules, electrons in solids exist in the environment formed by a crystal lattice

impurity scattering

low-temperature transport is typically dominated by potential disorder responsible for residual resistivity

electron-phonon scattering

high-temperature transport is determined by scattering off lattice vibrations - phonons

intermediate temperatures

$$\tau_{ee} \ll \tau_{\rm dis}, \tau_{\rm ph} \qquad\qquad T_{\rm dis} \ll T \ll T_{\rm ph}$$

hydrodynamic behavior is established by electron-electron interaction which may dominate in an intermediate temperature window, that is not guaranteed to exist

unconventional hydrodynamics in graphene

hydrodynamic approach to graphene

Briskot et.al (2015); Schütt, BN (2019); BN, Gornyi (2021)

Dirac fermions in graphene

linear spectrum

no Galilean invariance

momentum density proportional to energy current

classical (3D) Coulomb interaction

no Lorentz invariance

Vlasov-like self-consistency

non-degenerate Fermi gas
(close to the neutrality point)

temperature is the only energy scale

transition to a Fermi-liquid-like behavior at high carrier densities

continuity equations

particle number (*two bands!*)

$$\partial_t n + \boldsymbol{\nabla} \cdot \boldsymbol{j} = 0$$

$$\partial_t n_I + \boldsymbol{\nabla} \cdot \boldsymbol{j}_I = - \left[n_I - n_{I,0} \right] / \tau_R$$

energy density

$$\partial_t n_E + \boldsymbol{\nabla} \cdot \boldsymbol{j}_E = e\boldsymbol{E} \cdot \boldsymbol{j} - \left[n_E - n_{E,0} \right] / \tau_{RE}$$

momentum density

$$\partial_t n_{\boldsymbol{k}}^\alpha + \nabla_{\boldsymbol{r}}^\beta \Pi_E^{\alpha\beta} - enE^\alpha - \frac{e}{c} \left[\boldsymbol{j} \times \boldsymbol{B} \right]^\alpha = - \frac{n_{\boldsymbol{k}}^\alpha}{\tau_{\rm dis}}$$

$$\boldsymbol{j}_E = v_g^2 \boldsymbol{n}_{\boldsymbol{k}}$$

ideal hydrodynamics in graphene

Briskot et.al (2015), Schütt, BN (2019)

generalized Euler equation

$$\boldsymbol{j}_E = W\boldsymbol{u}$$

$$W(\partial_t + \boldsymbol{u}\cdot\boldsymbol{\nabla})\boldsymbol{u} + v_g^2\boldsymbol{\nabla}P + \boldsymbol{u}\partial_t P + e(\boldsymbol{E}\cdot\boldsymbol{j})\boldsymbol{u} = v_g^2 en\boldsymbol{E} + v_g^2\frac{e}{c}\boldsymbol{j}\times\boldsymbol{B} - \frac{W\boldsymbol{u}}{\tau_{\mathrm{dis}}}$$

linear response in degenerate limit

$$\boldsymbol{j} = n\boldsymbol{u} \quad \Rightarrow \quad v_g^2 en\boldsymbol{E} + v_g^2\frac{e}{c}\boldsymbol{j}\times\boldsymbol{B} = \frac{\mu\boldsymbol{j}}{\tau_{\mathrm{dis}}}$$

Drude-like resistivity

$$\rho^0_{xx} = \frac{\pi}{e^2|\mu|\tau_{\mathrm{dis}}} \qquad R_H^{(0)} = \frac{1}{nec}$$

charge-energy decoupling in neutral graphene

$$v_g^2\frac{e}{c}\boldsymbol{j}\times\boldsymbol{B} = \frac{\boldsymbol{j}_E}{\tau_{\mathrm{dis}}}$$

key to understand Wiedemann-Franz law violation in graphene

parabolic magnetoresistance

$$\delta R(B;\mu=0) = \mathcal{C}\frac{v_g^4}{c^2}\frac{B^2\tau_{\mathrm{dis}}}{T^3} \qquad R_H = 0$$

Müller, Sachdev (2008); BN et.al (2015)

thermal conductivity and Wiedemann-Franz law violation

neglecting viscosity and supercollisions and the related quasiparticle recombination; for review see Lucas, Fong (2018)

linear response currents

neglect viscosity and supercollisions

$$\tau_R \to 0 \quad \Rightarrow \quad \mu_I = 0; \qquad \eta \to 0$$

linear response

$$\boldsymbol{J} = e\left[\frac{v_g^2 \tau_{\rm dis} \bar{n}^2}{3\bar{P}} + \bar{\Sigma}_{11}\right]\left[e\boldsymbol{E} - T\boldsymbol{\nabla}\frac{\mu}{T}\right] - \frac{e v_g^2 \tau_{\rm dis} \bar{n}}{T}\boldsymbol{\nabla}T$$

$$\boldsymbol{Q} = \left[v_g^2 \tau_{\rm dis} \bar{n}\left(1 - \frac{\bar{\mu}\bar{n}}{3\bar{P}}\right)\right]\left[e\boldsymbol{E} - T\boldsymbol{\nabla}\frac{\mu}{T}\right] - \frac{v_g^2 \tau_{\rm dis}}{T}\left(3\bar{P} + \bar{\mu}\bar{n}\right)\boldsymbol{\nabla}T$$

kinetic coefficients

$$\sigma = e^2 \frac{v_g^2 \tau_{\rm dis} \bar{n}^2}{3\bar{P}} + e^2 \bar{\Sigma}_{11} \qquad \kappa = \frac{3\bar{P}}{\bar{T}} v_g^2 \tau_{\rm dis} \frac{e^2 \bar{\Sigma}_{11}}{\sigma}$$

Lorentz number at charge neutrality

conductivity

$$\sigma(\mu = 0) = e^2 \bar{\Sigma}_{11} = \frac{2\ln 2}{\pi} e^2 \bar{T} \frac{\tau_{11}\tau_{\rm dis}}{\tau_{11} + \tau_{\rm dis}} \to \mathcal{A}\frac{e^2}{\alpha_g^2}$$

thermal conductivity

$$\kappa(\mu = 0) \to \frac{3\bar{P}}{\bar{T}} v_g^2 \tau_{\rm dis} = \frac{18\zeta(3)}{\pi}\bar{T}^2 \tau_{\rm dis}$$

Lorentz number

$$L(\mu = 0) = \frac{27\zeta(3)}{\pi^2 \ln 2}\left(\frac{\tau_{\rm dis}}{\tau_{11}} + 1\right) L_0 = \mathcal{C}_0 L_0$$

$$\mathcal{C}_0(\alpha_g = 0.23,\ \tau_{\rm dis}^{-1} = 0.8\,\mathrm{THz},\ T = 298\,\mathrm{K}) = 53.4$$

Wiedemann-Franz law violation

measured Lorenz number in the hydrodynamic regime significantly deviates from the universal (FL) value

experiment in graphene

Kim group (2016)

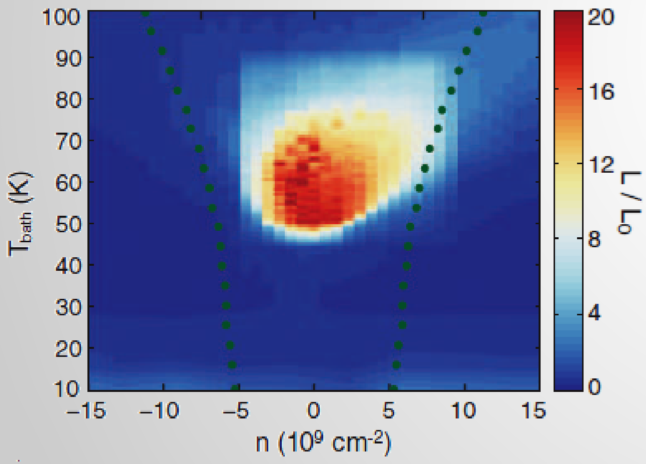

topological materials (WP_2, MoP)

Felser group (2018)

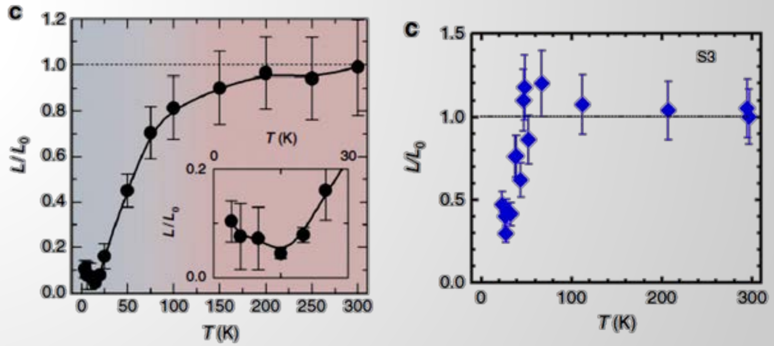

dissipative terms in graphene – electrical conductivity

Briskot et.al (2015); Schütt, BN (2019); BN, Gornyi, Titov (2021)

dissipative parts of the currents

electric and imbalance currents

$$\boldsymbol{j} = n\boldsymbol{u} + \delta\boldsymbol{j} \qquad\qquad \boldsymbol{j}_I = n_I\boldsymbol{u} + \delta\boldsymbol{j}_I$$

linear response

$$\begin{pmatrix} \delta\boldsymbol{j} \\ \delta\boldsymbol{j}_I \end{pmatrix} = \widehat{\Sigma} \begin{pmatrix} e\boldsymbol{E} - T\boldsymbol{\nabla}(\mu/T) \\ -T\boldsymbol{\nabla}(\mu_I/T) \end{pmatrix}$$

conductivity at charge neutrality

Kashuba (2008)

$$\sigma_Q(\mu{=}0) = \mathcal{A}\,\frac{e^2}{\alpha_g^2} \qquad \mathcal{A} \approx 0.12$$

conductivity matrix at zero magnetic field

$$\widehat{\Sigma} = \widehat{\mathfrak{M}}\,\widehat{\mathfrak{S}}_{xx}^{-1}\,\widehat{\mathfrak{M}}, \quad \widehat{\mathfrak{S}}_{xx} = \frac{\alpha_g^2 T^2}{2\mathcal{T}^2}\widehat{\mathfrak{T}} + \frac{\pi}{\mathcal{T}\tau_{\mathrm{dis}}}\widehat{\mathfrak{M}},$$

$$\widehat{\mathfrak{M}} = \begin{pmatrix} 1 - \frac{2\tilde{n}^2}{3\tilde{n}_E}\frac{T}{\mathcal{T}} & \frac{xT}{\mathcal{T}} - \frac{2\tilde{n}\tilde{n}_I}{3\tilde{n}_E}\frac{T}{\mathcal{T}} \\ \frac{xT}{\mathcal{T}} - \frac{2\tilde{n}\tilde{n}_I}{3\tilde{n}_E}\frac{T}{\mathcal{T}} & 1 - \frac{2\tilde{n}_I^2}{3\tilde{n}_E}\frac{T}{\mathcal{T}} \end{pmatrix}, \quad \widehat{\mathfrak{T}} = \begin{pmatrix} t_{11}^{-1} & t_{12}^{-1} \\ t_{12}^{-1} & t_{22}^{-1} \end{pmatrix}$$

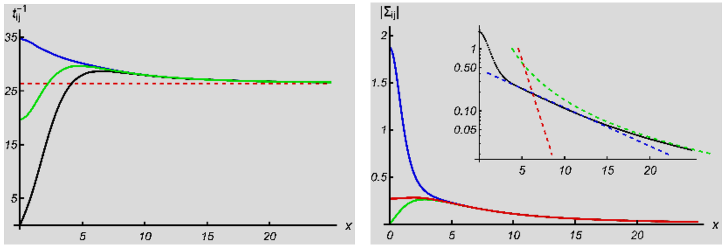

optical conductivity

optical conductivity in neutral graphene

Wang group (2019)

Quantum-critical scattering rates

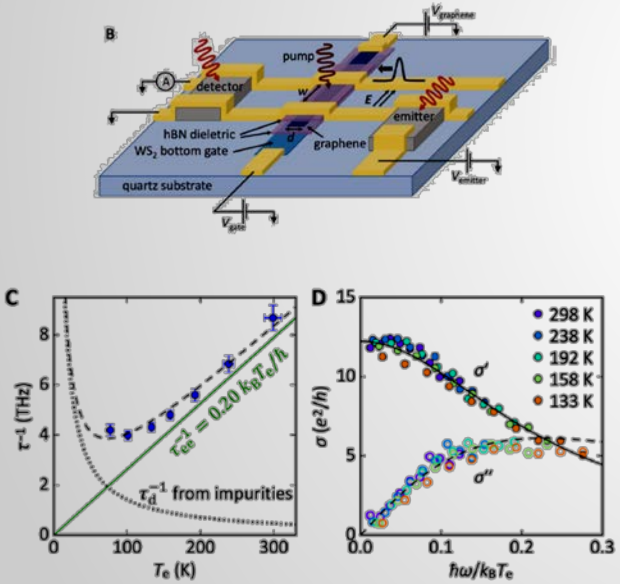

optical conductivity in hydrodynamics

hydrodynamic contribution

$$\sigma_h = \frac{e^2 v_g^2 n^2}{W} \frac{1}{\tau_{\rm dis}^{-1} - i\omega}$$

kinetic contribution

$$\sigma_k(\mu = 0) = \frac{2\ln 2}{\pi} \frac{e^2 T}{\tau_{\rm dis}^{-1} + \tau_{11}^{-1} - i\omega}$$

Sun, Basov, Fogler (2018); BN (2019)

$$\tau_{11}^{-1} \propto \alpha_g^2 T$$

Kashuba (2008); Fritz et.al (2008)

optical conductivity

optical conductivity measurements allow for an experimental analysis of microscopic scattering processes

bad metals

Delacretaz, Gouteraux, Hartnoll, Karlsson (2015)

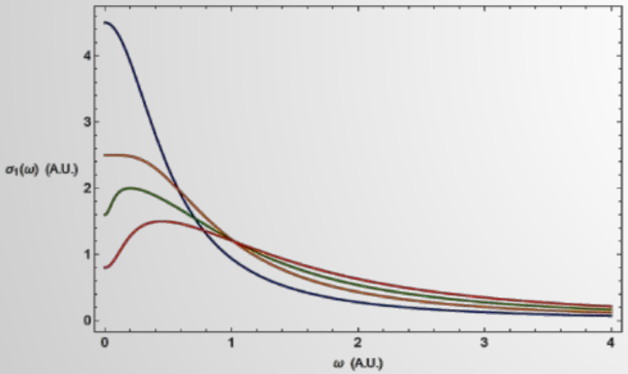

Figure 1: Illustrative plot of the temperature dependence of the optical conductivity of bad metals. As temperature is increased, the peak broadens and then moves off the $\omega = 0$ axis.

graphene in hydrodynamic regime

BN (2019)

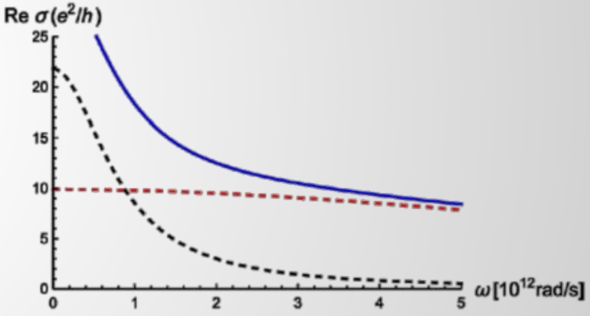

FIG. 2. Optical conductivity in weakly doped graphene at $n = 0.08\,\mathrm{cm}^{-12}$ [or $E_F = 33\,\mathrm{meV}$, the value used in Ref. [1]; see Fig. 4(b) of that reference]. The almost flat red dashed curve shows the real part of the kinetic contribution (15b), while the black dashed curve shows the real part of the hydrodynamic contribution (21). The real part of the full electrical conductivity (i.e., the sum $\delta\sigma + \sigma_h$) is shown by the solid blue curve. The curves were calculated with $\alpha_g = 0.23$, $T = 298\,\mathrm{K}$, and $\tau_{\mathrm{dis}}^{-1} = 0.8\,\mathrm{THz}$, the values taken from Ref. [1].

viscous flow of charge

dissipative terms in graphene - viscosity

Schütt, BN (2019)

viscosity in graphene

dissipative part of the stress tensor

$$\Pi_E^{\alpha\beta} = \Pi_{E,0}^{\alpha\beta} + \delta\Pi_E^{\alpha\beta},$$
$$\delta\Pi_E^{\alpha\beta} = -\eta(B)\mathfrak{D}^{\alpha\beta} + \eta_H(B)\epsilon^{\alpha ij}\mathfrak{D}^{i\beta}e_B^j,$$
$$\mathfrak{D}^{\alpha\beta} = \nabla^\alpha u^\beta + \nabla^\beta u^\alpha - \delta^{\alpha\beta}\boldsymbol{\nabla}\cdot\boldsymbol{u},$$

zero bulk viscosity

$$\zeta = 0$$

viscosity near charge neutrality

Müller et.al, (2009)

$$\eta(\mu=0) = \mathcal{B}\,\frac{T^2}{\alpha_g^2 v_g^2} \qquad \mathcal{B} \approx 0.45$$

viscosity in magnetic field

shear viscosity

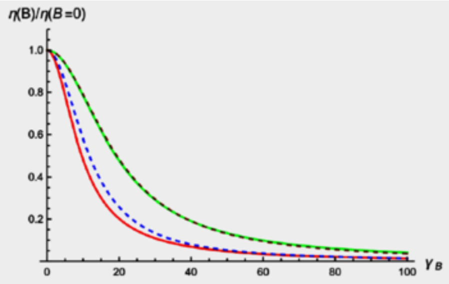

Hall viscosity

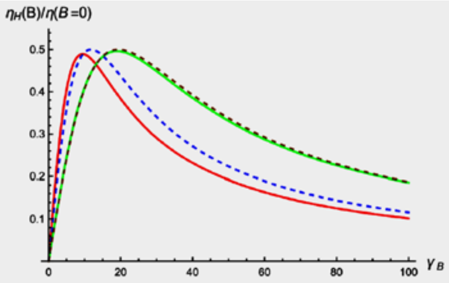

viscosity in graphene in the degenerate regime

model calculation yields good qualitative agreement with the data but overestimates the value

data from nonlocal transport

Geim group (2016)

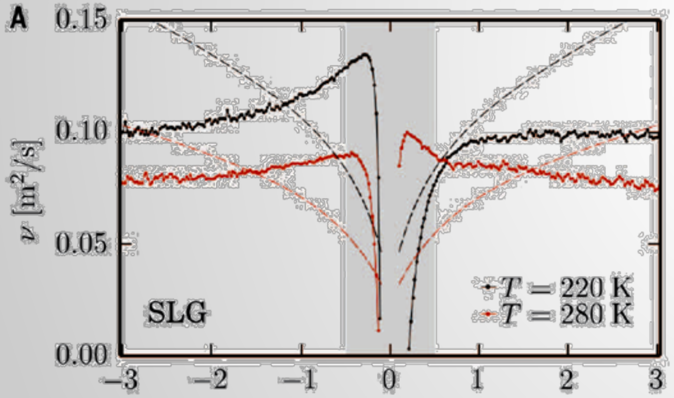

three-mode approximation

Schütt, BN (2019)

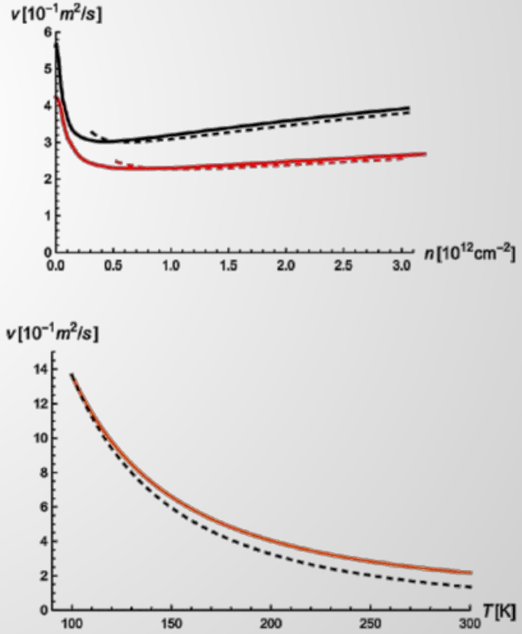

imaging of electronic flows

electronic flow in a narrow channel

local probes allow to determine local current density and uncover Poiseuille flows

scanning nanotube SET – doped graphene

Weizmann group (2019)

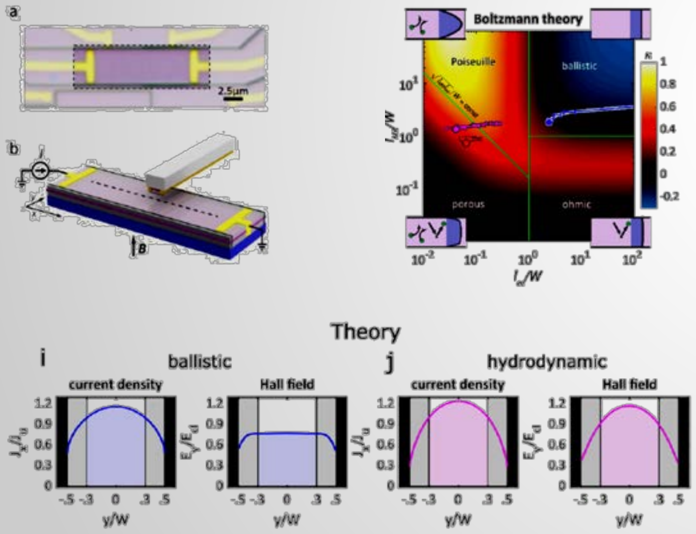

NV centers in diamonds – “Dirac fluid”

Harvard group (2020)

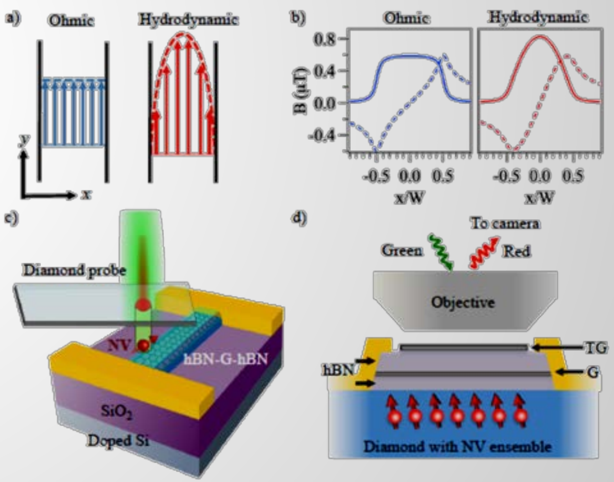

Poiseuille flow in doped graphene

nearly single-band electronic fluid is similar to conventional fluids and may exhibit Poiseuille-like flow

scanning nanotube SET – doped graphene

Weizmann group (2019)

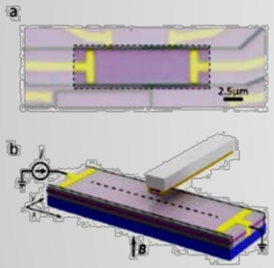

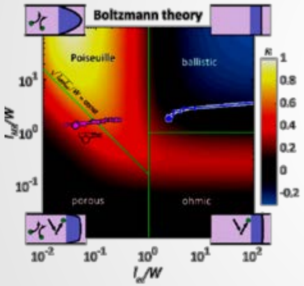

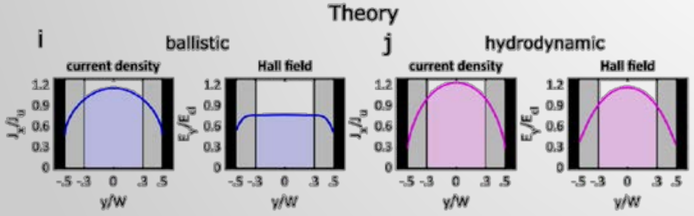

Poiseuille-like flow – catenary flow profile

Alekseev et.al (2018)

current density with no-slip boundary conditions

$$J_x = \sigma E_x \left[1 - \frac{\cosh(y/\ell_G)}{\cosh[W/(2\ell_G)]} \right]$$

Gurzhi length

$$\ell_G = \sqrt{\nu \tau_{\mathrm{dis}}}$$

Scaffidi et. al (2017); Pellegrino, Torre, Polini (2017);
Alekseev et.al (2018)

no-slip boundary conditions are unrealistic, but mixed (Maxwell's) boundary conditions lead to similar bulk behavior

Kiselev, Schmalian (2019)

electronic flow around an obstacle

Gusev et.al. (2020)

Poiseuille flow in a Hall bar (*GaAs*)

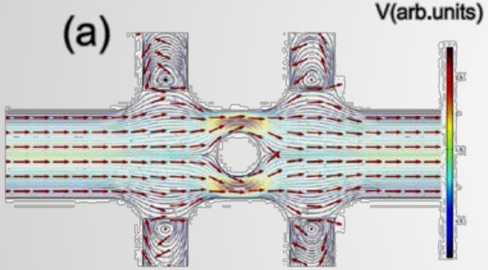

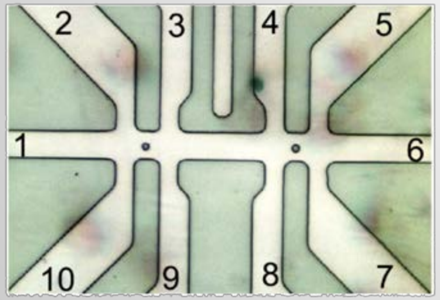

electron-electron relaxation rates

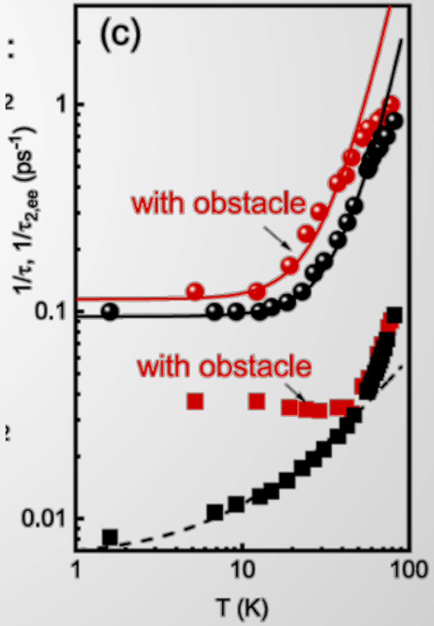

viscosity in graphene near charge neutrality

Schütt, BN (2019)

hydrodynamics at charge neutrality

electric current

$$\boldsymbol{j} = n\boldsymbol{u} + \delta\boldsymbol{j} = \delta\boldsymbol{j}$$

generalized Stokes (linear) equation

$$\boldsymbol{\nabla} P = \eta \Delta \boldsymbol{u} + \frac{e}{c}\delta\boldsymbol{j} \times \boldsymbol{B} - \frac{3P\boldsymbol{u}}{v_g^2 \tau_{\rm dis}}$$

in the absence of magnetic field, the electric current in neutral graphene is not hydrodynamic

BN, Gornyi, Titov (2021)

understanding of boundary conditions is key to interpret experimental data: channel geometry does not support Poiseuille flow!

viscosity at arbitrary densities

Harvard group (2020)

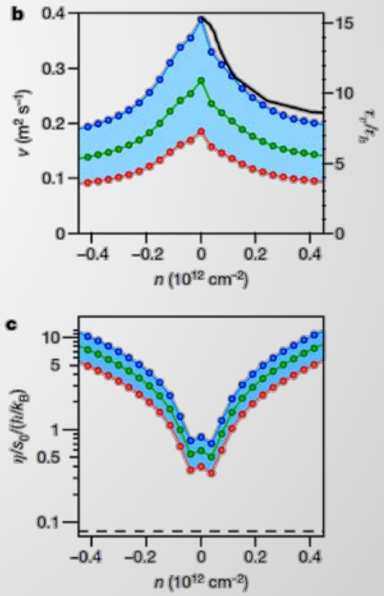

diffusive to ballistic crossover

in confined geometries, electron motion is governed by the ratio of the mean free path to the sample size

boundary conditions for distribution function

Beenakker, van Houten (1991)

slab geometry

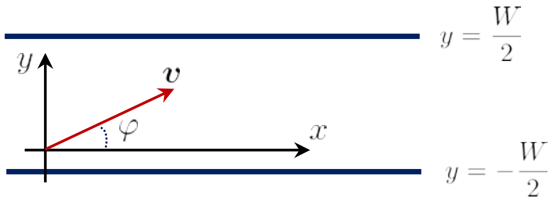

diffusive scattering at the boundary

$$f = f_0 + \delta f(y, \varphi)$$

$$\delta f\left(\frac{W}{2}; -\pi < \varphi < 0\right) = \frac{1}{2}\int_0^{\pi} d\varphi' \cos\varphi' \delta f\left(\frac{W}{2}; \varphi'\right)$$

outgoing *incoming*

current profile in the slab geometry

$$J_x \propto 4\int_0^1 dz\sqrt{1-z^2}\left[1 - e^{-\frac{1}{\ell z}}\cosh\frac{y}{\ell z}\right]$$

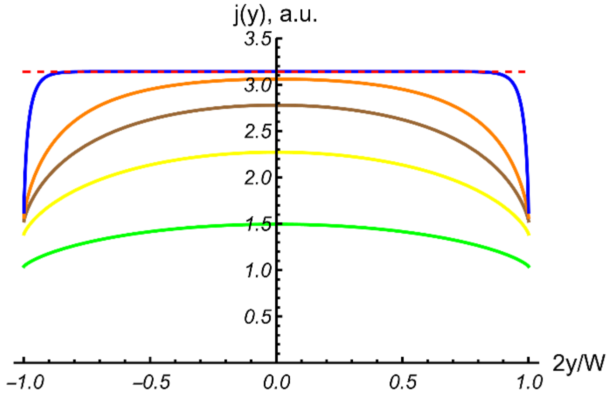

anti-Poiseuille flow in neutral graphene

in neutral graphene subjected to magnetic field the electronic flow is inhomogeneous

absence of Poiseuille flow in zero field

BN, Gornyi, Titov (2021)

absence of longitudinal hydrodynamic flow

$$\eta \frac{\partial^2 u_x}{\partial y^2} = \frac{3 P u_x}{v_g^2 \tau_{\rm dis}} \quad \Rightarrow \quad u_x = 0$$

Coulomb drag-like resistivity

$$\boldsymbol{J} = \frac{1}{R_0} \boldsymbol{E}, \qquad R_0 = \frac{\pi}{2 \ln 2} \frac{1}{e^2 T} \left(\frac{1}{\tau_{11}} + \frac{1}{\tau_{\rm dis}} \right)$$

Poiseuille-like flow of energy can be induced by applying a temperature gradient

Link, BN, Kiselev, Schmalian (2018)

anti-Poiseuille flow

BN, Gornyi, Titov (2021)

magnetic field couples the longitudinal current and lateral neutral quasiparticle (energy) flows leading to inhomogeneity

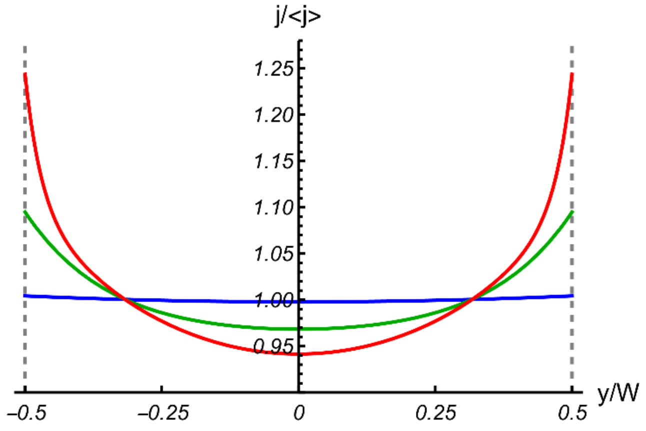

two-band phenomenology at charge neutrality

electron hydrodynamics in neutral graphene

Alekseev et.al, (2015)

edge vs bulk

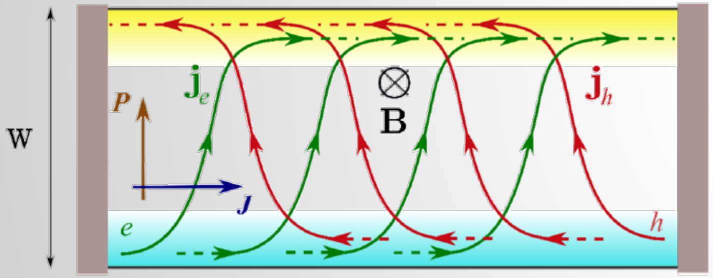

key to understand nonlocal transport experiments in graphene

linear magnetoresistance

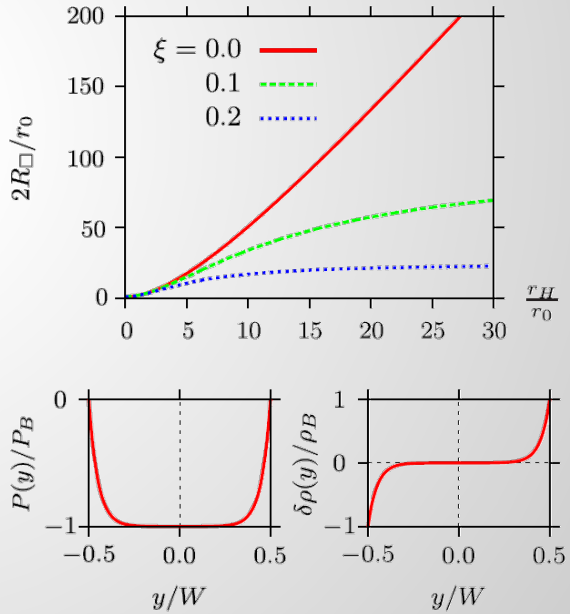

numerical solution of phenomenological equations

Danz, Titov, BN (2020)

two-band phenomenology

macroscopic currents (“Ohm’s Law”)

$$\boldsymbol{j} + eD(\nu_e + \nu_h)\boldsymbol{E} + \omega_c\tau\boldsymbol{j}_I \times \boldsymbol{e}_B + D\boldsymbol{\nabla}n = 0$$

$$\boldsymbol{j}_I + eD(\nu_e - \nu_h)\boldsymbol{E} + \omega_c\tau\boldsymbol{j} \times \boldsymbol{e}_B + D\boldsymbol{\nabla}\rho = 0$$

continuity equations

$$\boldsymbol{\nabla}\cdot\boldsymbol{j} = 0 \qquad \boldsymbol{\nabla}\cdot\boldsymbol{j}_I = -\frac{\delta\rho}{\tau_R}$$

Vlasov selfconsistency (gated structure)

$$\boldsymbol{E} = \boldsymbol{E}_0 - \frac{e}{C}\boldsymbol{\nabla}n$$

degenerate regime (single band)

Ohmic flow in the absence of magnetic field

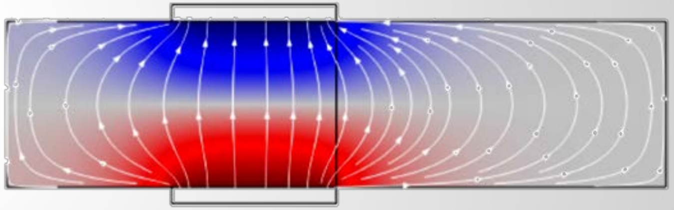

classical Hall effect

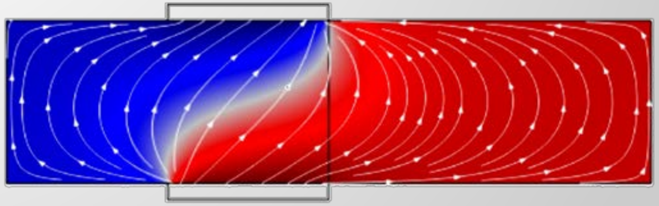

numerical solution of phenomenological equations

Danz, Titov, BN (2020)

two-band phenomenology

macroscopic currents (“Ohm’s Law”)

$$\boldsymbol{j} + eD(\nu_e + \nu_h)\boldsymbol{E} + \omega_c \tau \boldsymbol{j}_I \times \boldsymbol{e}_B + D\boldsymbol{\nabla} n = 0$$

$$\boldsymbol{j}_I + eD(\nu_e - \nu_h)\boldsymbol{E} + \omega_c \tau \boldsymbol{j} \times \boldsymbol{e}_B + D\boldsymbol{\nabla} \rho = 0$$

continuity equations

$$\boldsymbol{\nabla} \cdot \boldsymbol{j} = 0 \qquad \boldsymbol{\nabla} \cdot \boldsymbol{j}_I = -\frac{\delta\rho}{\tau_R}$$

Vlasov selfconsistency (gated structure)

$$\boldsymbol{E} = \boldsymbol{E}_0 - \frac{e}{C}\boldsymbol{\nabla} n$$

charge neutrality (two bands)

Ohmic flow in the absence of magnetic field

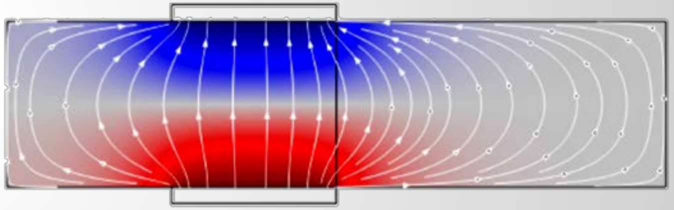

nonlocality in magnetic field

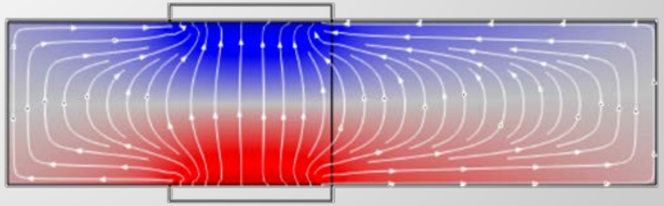

numerical solution of phenomenological equations

Danz, Titov, BN (2020)

nonlocal response: current density

Ohmic flow in the absence of magnetic field

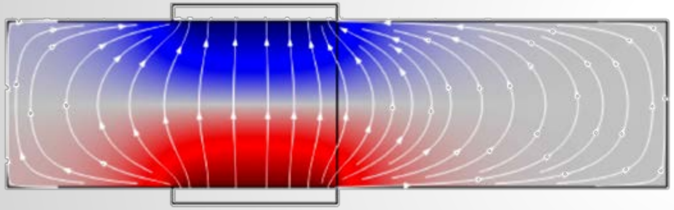

nonlocality on magnetic field

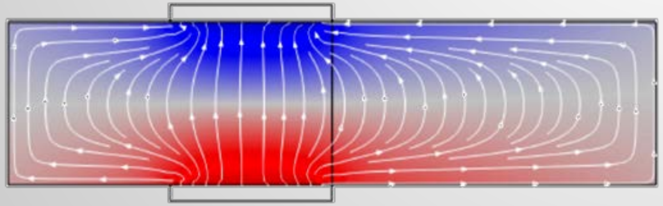

nonlocal resistance

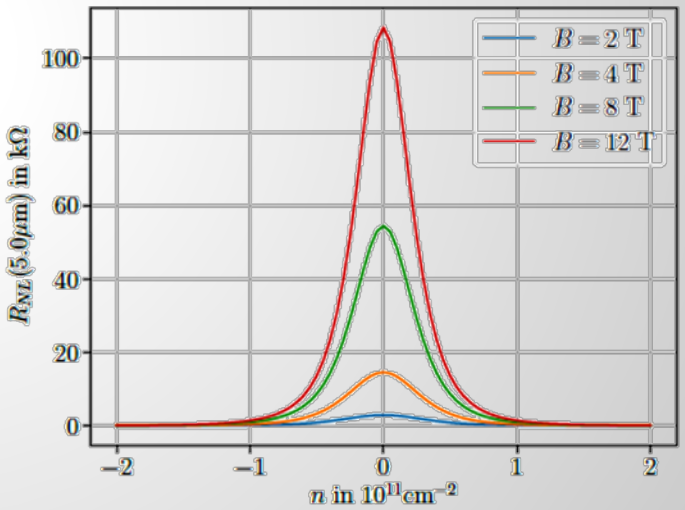

nonlocal resistance

vorticity, ballistic motion, or edge charge accumulation?

nonlocal transport in graphene

initial attempt at detecting non-uniform current flows

degenerate regime: negative local resistance

Geim group (2016)

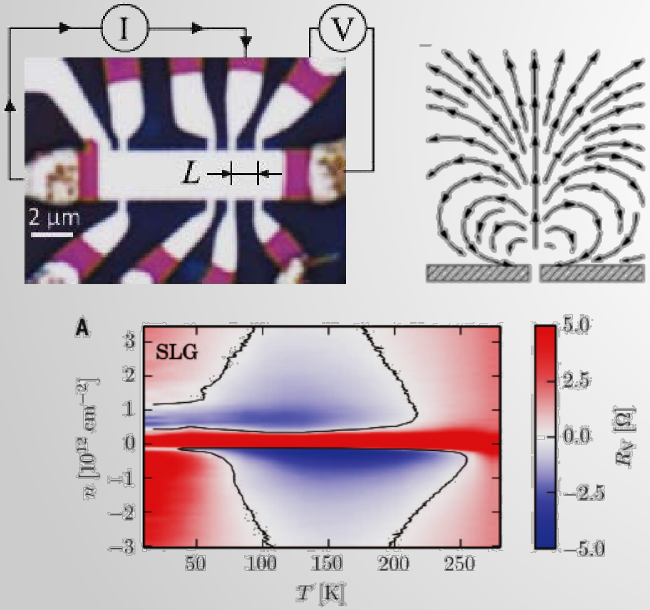

neutral graphene: giant nonlocality

Geim group (2011)

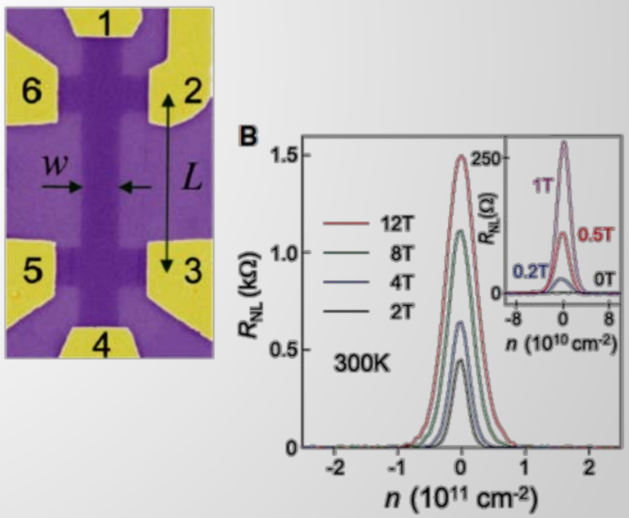

effect of viscosity on electron flow in doped graphene

results of nonlocal transport measurements can be interpreted with the help of a hydrodynamic approach; negative vicinity resistance can be attributed to vorticity of the electronic fluid.

Poiseuille flow

Torre, Tomadin, Geim, Polini (2015)

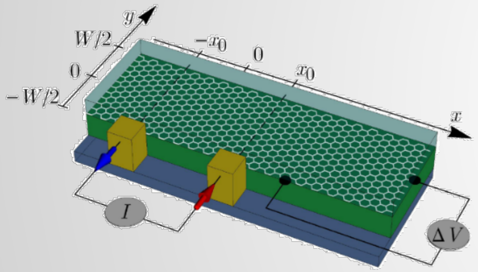

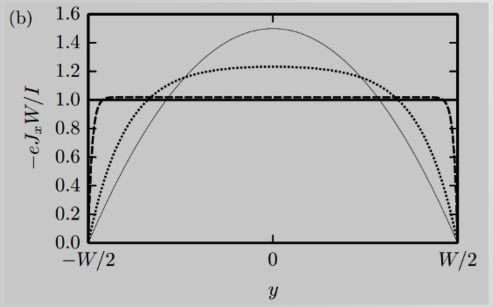

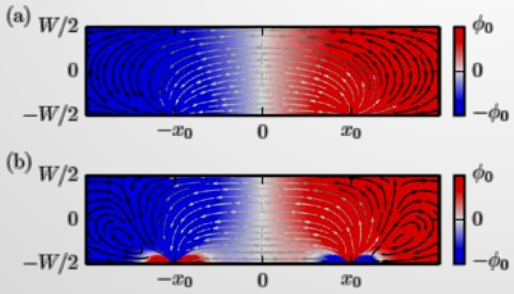

Ohmic vs viscous flow

Levitov, Falkovich (2016)

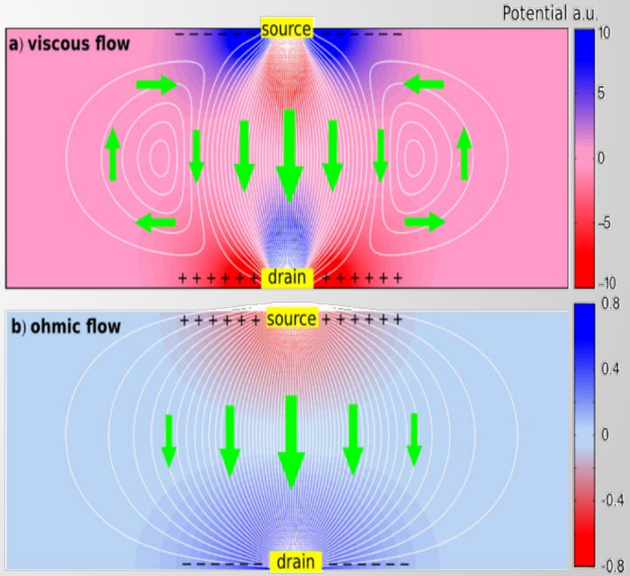

numerical solution of hydrodynamic equations

Danz, BN (2020)

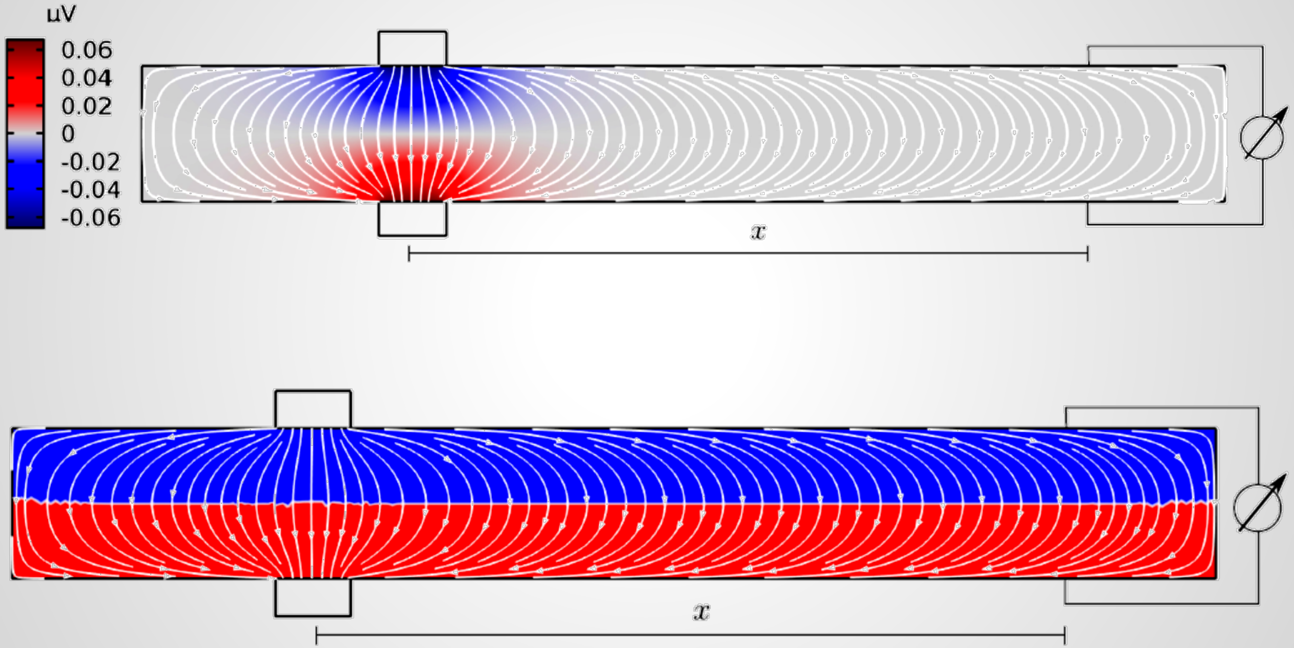

numerical solution of hydrodynamic equations

Danz, BN (2020)

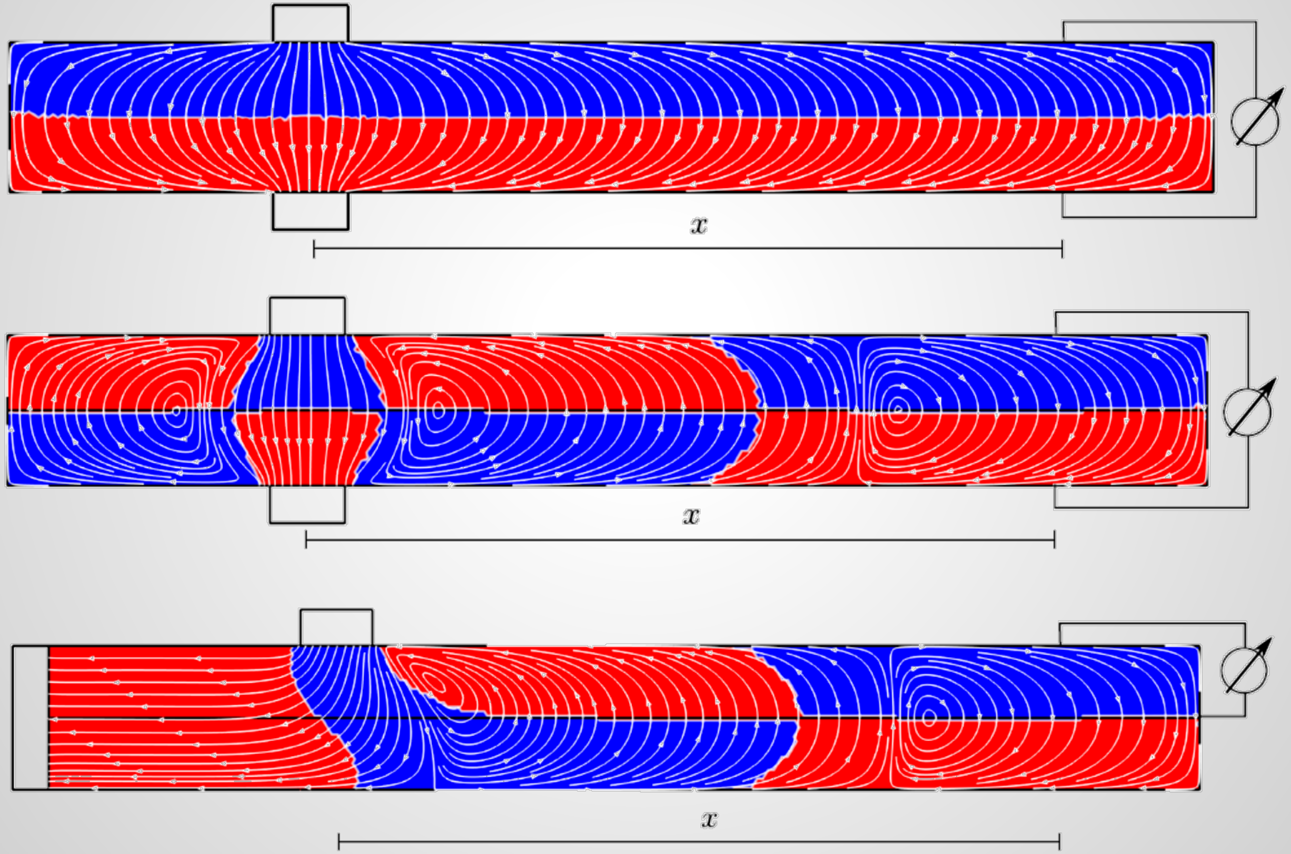

edge currents due to edge charge accumulation

classical edge physics may be masking more interesting bulk phenomena; Zeldov group (2020)

edge charge accumulation

band bending

electrostatic gating

charged impurities

LDoS in G/hBN wire (DFT)

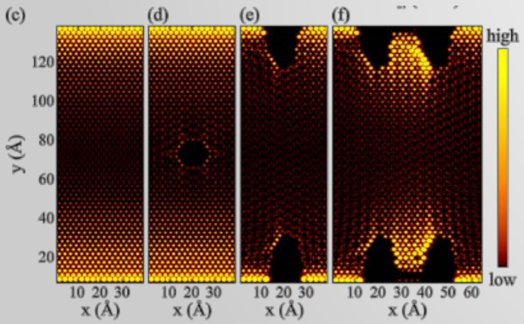

Marmolejo-Tejada et.al (2018)

Quantum Hall edge state

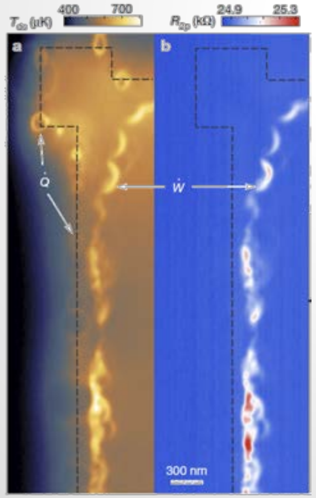

Marguerite et.al (2019)

experimental observations

non-decaying non-topological edge current in magnetic field *(leading to nonlocal transport)*

local potential *(scanning tip)* *is able to stop the edge current*

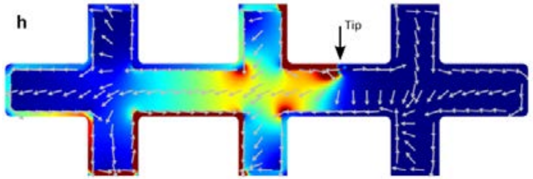

conclusions

electronic hydrodynamics: not boring, not 100% clear

experimental puzzles

nonlocal transport : bulk vs edge

low Lorentz numbers in topological materials

no “smoking gun”?

conjectured generalizations

universal linear resistivity

why should different materials saturate the proposed bounds?

what is the mechanism behind splitting into charge and energy modes?